

Reviews and syntheses: Photosynthetic oxygen evolution in plants-A potential inheritance from early abiotic oxygen production on Earth

Yanyou Wu^{1,*†}, Mohamed Aboueldahab^{1,2,†}, Congqiang Liu^{3,*}

¹State Key Laboratory of Environmental Geochemistry, Institute of Geochemistry, Chinese Academy of Sciences, 550081, Guiyang, China

² University of Chinese Academy of Sciences, 100049, Beijing, China

³School of Earth System Science, Tianjin University, 300072, Tianjin, China

*Correspondence: wuyanyou@mail.gyig.ac.cn (Yanyou Wu), liucongqiang@tju.edu.cn (Congqiang Liu)

†These authors should be considered co-first authors.

Abstract. The phenomenon of photosynthetic oxygen evolution by plants, as the basis of life on our planet, has long attracted scientists from various disciplines. This process converts natural solar energy and inorganic carbon into organic matter and oxygen, which are not only crucial for maintaining terrestrial ecosystems but also reveal the early evolution of the Earth's biosphere. In this review, we present evidence from various disciplines, such as paleontology, biochemistry, stratigraphy, geochemistry, and molecular evolutionary biology, to support the proposition that abiotic processes generated the earliest detected oxygen on Earth. The photodecomposition of bicarbonate (HCO_3^-) under sunlight, which releases oxygen and carbon dioxide in photosynthetic organisms, is, in our opinion, an inheritance of the abiotic oxygen release mechanism. In contrast, the water photolytic oxygen release mechanism evolved in response to the insufficient availability of inorganic carbon sources ($\text{CO}_2/\text{HCO}_3^-$) in the environment. This review provides insights into the evolution of oxygen production mechanisms and their implications for the design of artificial photosynthetic reactors.

1 Background and Challenge

Oxygenic photosynthesis, originating in cyanobacteria and spreading to green algae and plants, is a key event in Earth's geological and biological history (Hohmann - Marriott and Blankenship, 2011). This process significantly changed the planet's atmosphere, introducing free oxygen and triggering the Great Oxidation Event (GOE), which enabled the rise and diversification of

complex, oxygen-dependent life (Schirrmeister et al., 2013). The current consensus suggests that photosynthetic oxygen originates from water. However, recent evidence, including the bicarbonate effect, pH-dependent thylakoid carbonic anhydrase activity, photosystem II (PSII) crystalline structure insights, and re-evaluated heavy oxygen isotope labeling experiments, indicates that both water and bicarbonate photolysis contribute to photosynthetic oxygen generation. Examining bicarbonate photolysis thermodynamic efficiency, photosynthetic stoichiometry, the global water-carbon cycle, and the Dole effect reveals bicarbonate photolysis as a fundamental process, equally significant to water photolysis in photosynthetic oxygen evolution (Wu, 2021; 2023; Guo et al., 2024).

The evolution of photosynthetic organisms is inherently tied to the escalation of atmospheric oxygen. As described in Fig.1, Earth has experienced two GOEs: the first, 2.4-2 billion years ago, marked by cyanobacteria's emergence, saw atmospheric oxygen levels gradually rise to 1-2% of modern levels. Following this initial GOE, oxygen concentrations likely plateaued until about 850 million years ago, after which they ascended to approximately 20% of present atmospheric levels, with potential spikes to 30–35% during the Carboniferous era. The second GOE is closely associated with the proliferation of photosynthetic eukaryotes, which substantially enhanced photosynthesis and witnessed a notable increase in algal and lichen productivity, especially in terrestrial environments (Holland, 2006). Elevated atmospheric O₂ levels during the Carboniferous (~360–300 Ma) coincided with vascular plant evolution and enhanced carbon sequestration (Berner, 1999). Currently, the rise in atmospheric O₂ levels is correlated with cyanobacteria's emergence, leading scientists to conclude that aerobic photosynthesis independently originated within these taxa (Fischer et al., 2016; Hohmann - Marriott and Blankenship, 2011).

However, the previous conclusion hinges on the premise that significant abiotic oxygen sources were absent in the early Earth's atmosphere (Fischer et al., 2016). Recently, researchers studying the Clarion-Clipperton Zone's seafloor ecosystem have discovered that polymetallic nodules in ancient sediment layers 4000 meters deep emit considerable oxygen (Sweetman et al., 2024). This challenges the idea that early Earth lacked significant abiotic oxygen sources. Moreover, photosynthesis is a derived trait in extant taxa, including cyanobacteria, phylogenetically (Fischer et al., 2016). Challenging the view that aerobic photosynthesis originated exclusively in cyanobacteria, we hypothesize that it may have evolved from early

abiotic oxygen-generating processes, with bicarbonate photolysis being an inherited trait from primitive Earth's abiotic oxygen production mechanisms shown in Fig. 2. This review critically examines the hypothesis across three key domains: early abiotic oxygen production, the potential ancestry of PSII, and the two-substrate photosynthetic oxygen evolution.

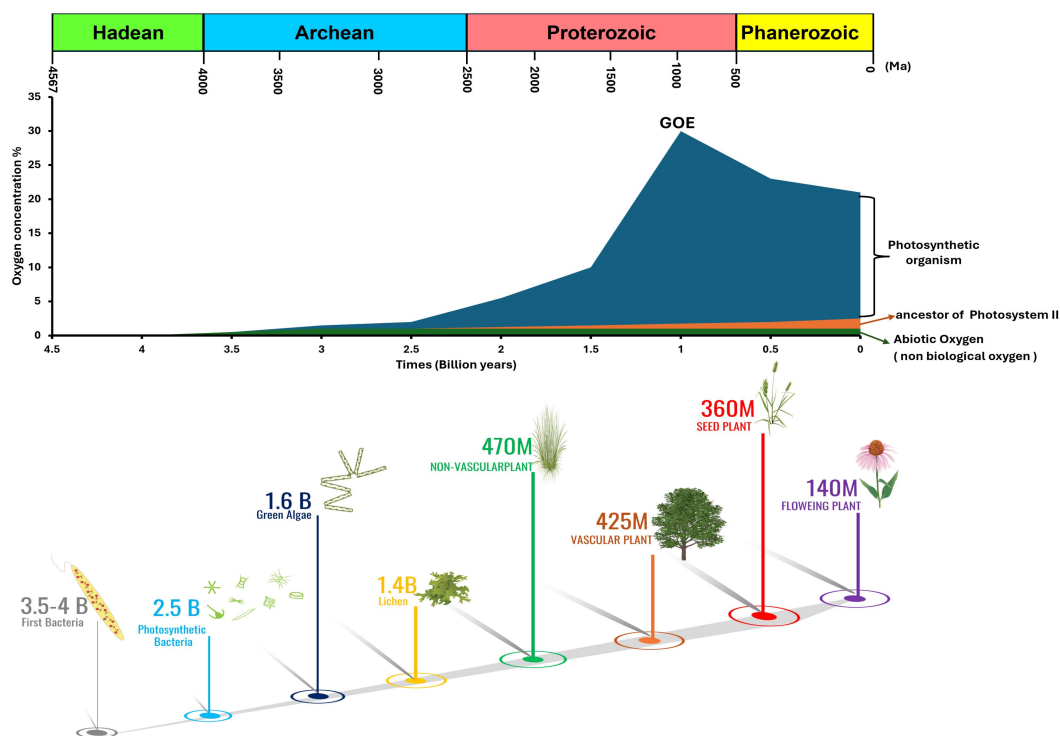


Figure 1. The connection between oxygen levels in Earth's atmosphere, the evolutionary milestones in plant life, and the early processes that contributed to oxygen generation. Here, we highlight the role of abiotic oxygen-generating processes before the emergence of biological oxygen production. The enzyme carbonic anhydrase is suggested as a potential precursor to PS II, a key component of the photosynthetic process responsible for oxygen production. It also depicts the evolution of the two-substrate photosynthetic oxygen-evolving process, which is critical for the significant rise in oxygen levels, particularly during the Great Oxidation Event (GOE), which leads to the diversification of complex plant life.

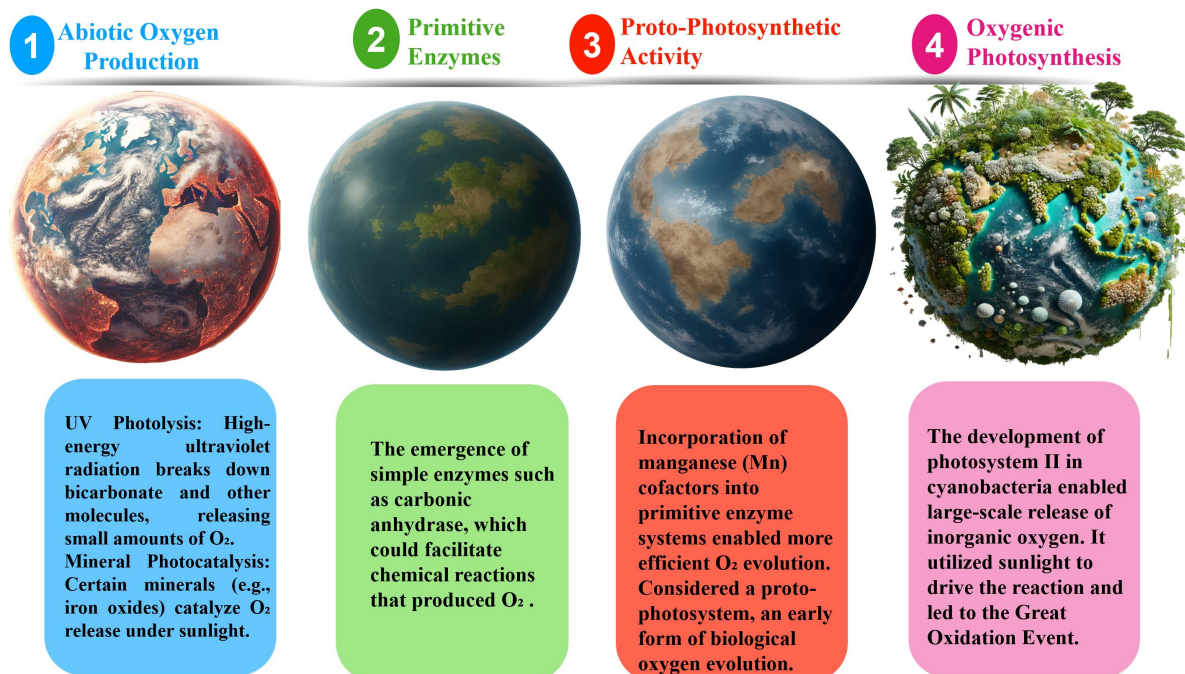


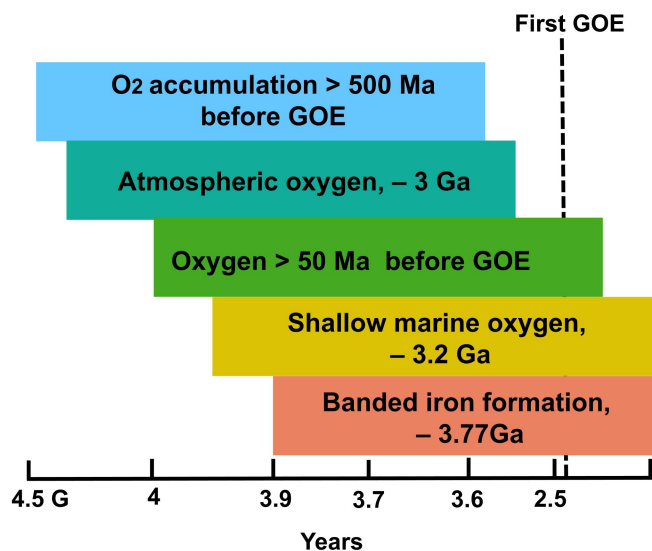
Figure 2. Conceptual diagram of the transition from abiotic to biotic oxygen evolution. Early Earth's abiotic processes (UV photolysis, mineral photocatalysis) produced small O_2 amounts (left), later augmented by primitive enzymes like carbonic anhydrase. Integrating Mn cofactors into such enzymes led to proto-photosynthetic activity (middle), eventually giving rise to the Mn-based photosystem II in cyanobacteria. This enabled large-scale bicarbonate/water splitting and oxygenic photosynthesis, fueling the rise of atmospheric oxygen and complex life (right). Each box represents a stage in the evolution of O_2 production.

2 Early abiotic oxygen production

Earth originated ~4.5 Ga ago, cooling ~100 Ma post-formation, leading to rock genesis (Wilde et al., 2001). Despite a significant rise in atmospheric O_2 levels during the first GOE, ~2.5-2.3Ga ago, studies of redox-sensitive trace elements and isotopes in Archean sedimentary (metamorphic) rocks suggest the presence of O_2 several hundred million years, or possibly over a billion years, before the emergence of photosynthetic cyanobacteria as illustrated in Fig. 3 (Fischer et al., 2016; Hohmann-Marriott and Blankenship, 2011; Xiong and Bauer, 2002).

Investigations into interstratified Fe and Ca-carbonate minerals within thick carbonate platforms (~2.9-2.8 Ga) of Canada's western Superior Province suggest that dynamic chemoclines, driven by oxygenic processes at platform edges, were common in the Archean eon. Dissolved

96 iron oxidation likely significantly influenced marine Ca-carbonate precipitation during that era
 97 (Riding et al., 2022). Isotopic analysis of Mo in rocks from the ~2.95 Ga Sinqeni Formation,
 98 Pongola Supergroup, South Africa, indicates that O₂ accumulation in shallow marine
 99 environments commenced >500 Ma before the first GOE shown in Fig. 3 (Planavsky et al., 2014).
 100 Additionally, high-resolution chem-stratigraphic analyses of redox-sensitive metals (Mo, Re) in
 101 the late Archean Mount McRae Shale, Western Australia, suggest their introduction to Archean
 102 oceans via oxidative weathering of crustal sulfides. This implies the existence of minimal oxygen
 103 levels >50 Ma prior to the first GOE (Anbar et al., 2007). Moreover, chromium isotope and
 104 redox-sensitive metal studies in the ~3-Ga-old Nsuze palaeosol and Ijzermyn iron formation
 105 (Pongola Supergroup) indicate significant atmospheric oxygen presence at that epoch shown in
 106 Fig. 3 (Crowe et al., 2013). An in-depth analysis of the Manzimnyama Banded Iron Formation
 107 (BIF) from South Africa's Fig Tree Group indicates substantial oxygen levels in shallow marine
 108 environments ~3.2 Ga ago (Satkoski et al., 2015). Lastly, iron isotope analysis from the Isua
 109 Supracrustal Belt (ca. 3.77 Ga) in West Greenland suggests that iron oxidation played a pivotal
 110 role in BIF deposition at that time (Czaja. et al., 2013).



111
 112
 113 **Figure 3.** Timeline of early abiotic oxygenation events prior to the Great Oxidation Event (GOE).
 114 Geochemical and isotopic evidence indicates that oxygen accumulation in Earth's environments
 115 began over 500 million years before the GOE (~2.5–2.3 Ga). Trace metal signatures (Mo, Re, Cr),
 116 iron isotopes, and banded iron formations (BIFs) reveal early oxygenic activity in shallow marine

environments (~3.2 Ga), atmospheric oxygen signals (~3.0 Ga), and oxygen-influenced BIF deposition as early as ~3.77 Ga. These findings suggest that localized oxygen production and redox cycling significantly predated the rise of oxygenic photosynthesis.

Despite the presence of oxygen since 3.8 Ga ago in the Archean eon, there remains considerable debate among scientists on whether the oxygen from that era to the rise of cyanobacteria 2.35 Ga ago was biologically generated throughout 1.4 Ga. The argument for oxygen generation by biological processes during this period is mainly supported by carbon isotope evidence and fossil records as described in Fig. 4. For example, researchers have found metamorphosed pelagic shale in West Greenland, dating to 3.7 Ga ago, with reduced carbon exhibiting $\delta^{13}\text{C}$ values as low as -25.6‰ PeeDee Belemnite (PDB) (Rosing and Frei, 2004). Additionally, negative $\delta^{13}\text{C}$ values have been traced in organic matter from sedimentary rocks as old as 3.8 Ga (Schidlowski, 1988). Investigations of 2.724-Ga-old Tumbiana Formation stromatolites from Australia's Fortescue Group have shown that their thin layers' clusters of organic globules strikingly resemble organic-mineral structures in modern stromatolites (Lepot et al., 2008). Additionally, research on the 3.465-Ga-old Apex chert from the Warrawoona Group, Western Australia, has revealed 11 filamentous structures resembling cyanobacterial microfossils (Brasier et al., 2005; Schopf, 1993; Schopf and Packer, 1987). Furthermore, investigations of sedimentary rocks from the Barberton Supergroup in the Barberton Mountains of South Africa have identified numerous filamentous structures resembling cyanobacteria-like microorganisms at two distinct stratigraphic levels within the 3.5-Ga-old Onverwacht Group (Walsh and Lowe, 1985).

Increasing research has raised questions about the reliability of interpreting Archean carbon isotopes and microfossil evidence as indicators of oxygen emergence (Fischer et al., 2016; Hohmann-Marriott and Blankenship, 2011). Negative $\delta^{13}\text{C}$ values are also present in organic compounds generated in numerous geological environments (McCollom and Seewald, 2006); moreover, the genetic machinery for carbon fixation is not exclusive to photosynthetic organisms (Lindell et al., 2005). Extensive analysis of microfossil-like structures found in 3.465-Ga-old Apex chert from the Warrawoona Group in Western Australia employed advanced techniques, including optical and electron microscopy, micro-Raman spectroscopy, etc.. These formations, previously identified as "microfossils" in metalliferous hydrothermal vein chert and volcanic glass,

are now recognized as "pseudofossils". They form from carbonaceous material reorganization during amorphous silica's recrystallization into spheroidal structures. It is plausible that carbon isotopes in Apex chert's carbonaceous material experienced fractionation within hydrothermal systems (Brasier et al., 2002; 2005). Furthermore, given hydrothermal and groundwater alterations in Apex chert, it is unlikely that it preserved early life forms (Pinti et al., 2009). Microscopic and Raman spectroscopic analyses of microfossils in Apex chert reveal filaments as mere quartz and hematite-filled cracks, with carbonaceous matter dispersed in the surrounding quartz matrix and not associated with these fissures (Marshall et al., 2011). Thus, oxygen presence before the first GOE likely resulted from abiotic geological processes of the Archean eon, not from oxygenic photosynthesis.

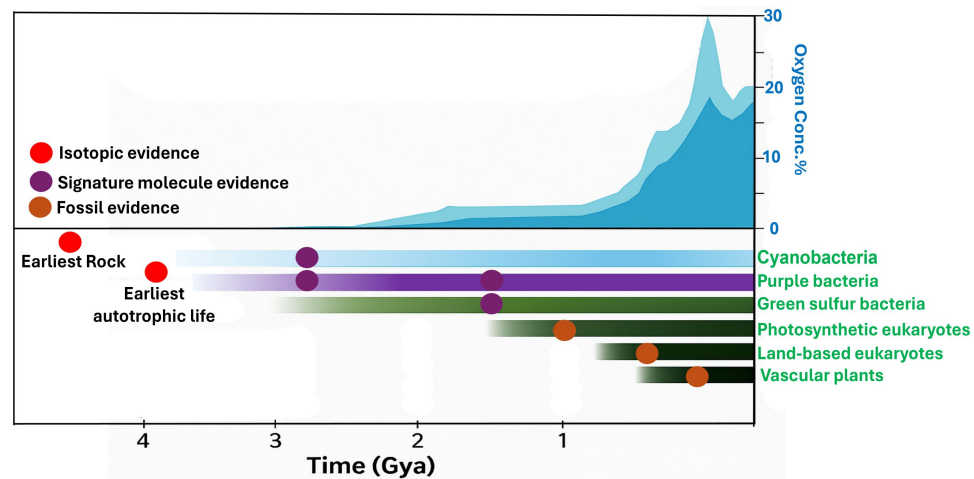


Figure 4. The Earth's geological history is linked to the emergence and evolution of photosynthesis. As labelled in the original publication (Hohmann-Marriott and Blankenship 2011), "minimum and maximum estimates for oxygen concentration are indicated by dark blue and light blue areas, respectively. The timeline highlights the appearance of major phototrophic and eukaryotic lineages alongside geochemical and fossil evidence, including isotopic (red), molecular biomarker (purple), and fossil (orange) signals. While early records such as isotopic signatures and purported microfossils from the Apex chert (~3.465 Ga) have been used to infer early life and oxygenic activity, recent studies challenge their biogenic origin. These "pseudofossils" and ambiguous $\delta^{13}\text{C}$ values underscore the complexity of interpreting early biosignatures, as similar carbon isotope fractionation can occur in abiotic hydrothermal systems.

Land-based geological light-capturing systems and 'dark' oxygen production on the deep ocean floor provide stronger evidence for abiotic oxygen release. Land's geological light-capturing systems and "dark" oxygen on the deep ocean floor provide stronger evidence for abiotic oxygen release (Lu et al., 2019; Sweetman et al., 2024). Scientists employed electron microscopy, X-ray absorption spectroscopy, and micro-Raman spectroscopy to investigate semiconducting iron and manganese (oxyhydroxy) oxide mineral coatings on rock and soil surfaces. They discovered that these oxyhydroxy coatings function as "photoelectric devices," capable of absorbing light and converting it into electricity (Lu et al., 2019). In-situ benthic chamber experiments at 4,000m depth in the Pacific revealed that polymetallic nodules can markedly enhance oxygen levels, tripling ambient concentrations within 48 hours. Furthermore, these nodules displayed high voltage potentials, reaching up to 0.95V shown in Fig.5 (Sweetman et al., 2024).

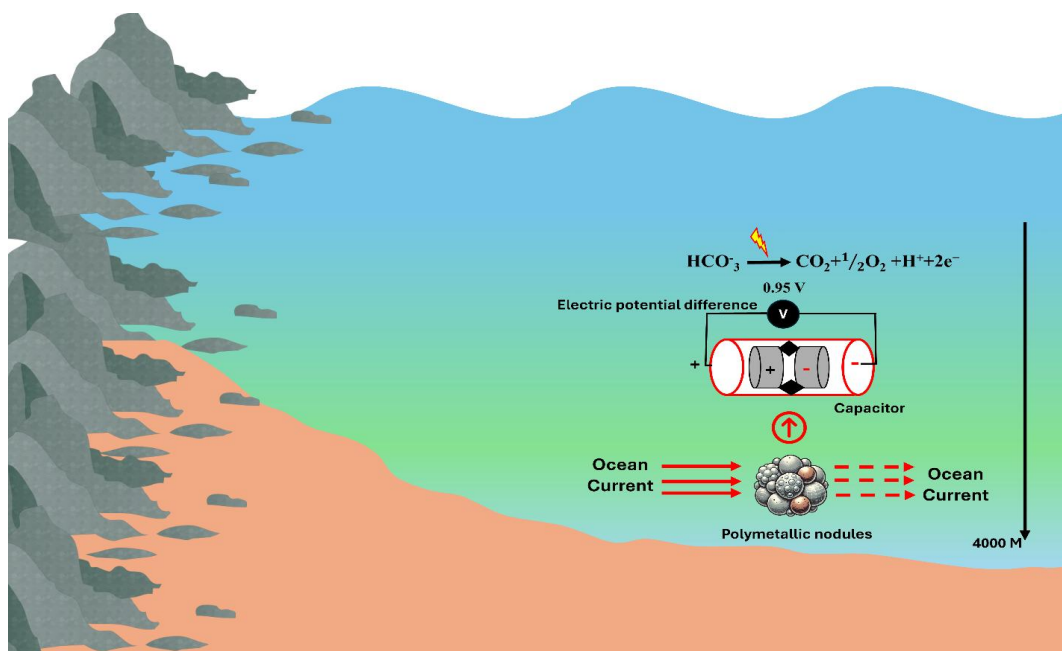


Figure 5. A schematic model showing the role of deep-sea polymetallic nodules, which act as energy storage systems, akin to capacitors, in the presence of ocean currents and hydrodynamic forces. The ocean currents flowing over the surface of these nodules generate an electric potential difference, as shown in 0.95 V. Although this voltage is insufficient to drive water molecule decomposition (which requires about 1.5 V), it is enough to facilitate the decomposition of HCO_3^- . This reaction leads to the release of O_2 and CO_2 . The process highlights an abiotic pathway for

oxygen generation, suggesting that non-biological sources of oxygen could have existed during the Archean eon. This discovery broadens our understanding of early Earth's oxygen generation mechanisms, indicating that these nodules may have contributed to oxygen production before the rise of biological photosynthesis.

Sunlight interaction with iron-manganese oxide "mineral coatings" on rocks facilitates a non-biological oxygen generation pathway. These semiconducting mineral layers absorb solar radiation, producing photoelectrons that catalyze redox reactions, transforming light into chemical energy. This enables the photo-catalytic breakdown of water or bicarbonate ions, yielding oxygen (Lu et al., 2019). Furthermore, polymetallic nodules on the abyssal seafloor serve as unique electrochemical reactors. Exposed to ocean currents and hydrodynamic forces, they harness various energy inputs on their surfaces, effectively functioning as capacitor (Wang et al., 2021). The generated surface voltage, inadequate for direct water molecule decomposition (~1.5 V needed) (Sweetman et al., 2024), but suffices for bicarbonate ion dissociation, resulting in oxygen release shown in Fig. 6 (Dismukes et al., 2001). This implies that non-biological O₂ sources were likely prevalent on Earth during the Archean eon. Absence of definitive carbon isotope and microfossil evidence from this era suggests that significant non-biological O₂ sources lend robust support to the hypothesis that O₂ existed pre-GOE. Furthermore, non-biological O₂ production mechanisms are akin to those of photosynthetic organisms. Moreover, organic carbon from non-biological processes shows isotopic traits similar to photosynthetic assimilation (McCollom and Seewald, 2006).

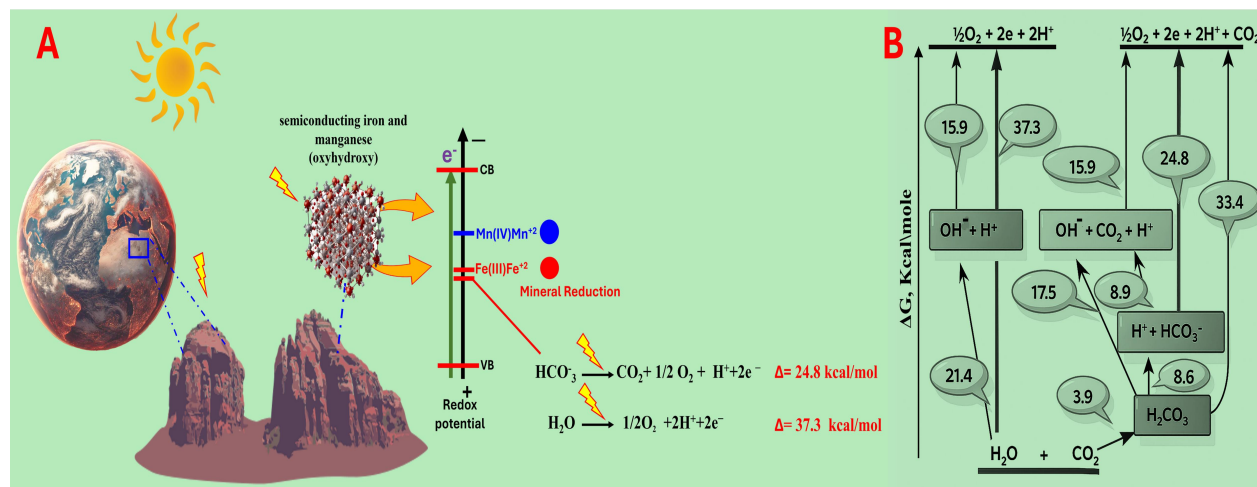


Figure 6. A conceptual model illustrating the light-driven abiotic oxygen release mechanism via semiconducting iron and manganese (oxyhydroxide) mineral coatings at the Earth's surface. This schematic highlights how sunlight interacts with these mineral coatings, commonly found on terrestrial rocks, to initiate redox reactions and release oxygen, a potential precursor to biological photosynthesis. Sunlight excites electrons (e^-) in the semiconducting iron and manganese oxides, elevating them from the valence band (VB) to the conduction band (CB). This electron excitation creates a redox potential sufficient to reduce Fe^{3+} to Fe^{2+} and Mn^{4+} to Mn^{2+} , as indicated by the energy levels on the right. Simultaneously, the photogenerated holes facilitate the oxidation of bicarbonate (HCO_3^-) and water (H_2O), resulting in the release of molecular oxygen (O_2) and carbon dioxide (CO_2), with respective energy changes of $\Delta = 24.8$ kcal/mol for bicarbonate and $\Delta = 37.3$ kcal/mol for water. These mineral-mediated photolysis reactions represent a purely abiotic oxygen production pathway, active during the Archean eon, long before the emergence of biological photosynthesis. Notably, this pathway expands the traditional view of solar energy utilization beyond the organic biosphere (plants and microbes), incorporating the geosphere's inorganic, semiconducting materials as functional participants in Earth's early redox and atmospheric evolution. In this context, Fe and Mn oxides serve as photoactive platforms that catalyze electron transfer and oxygen evolution, mechanistically mimicking the light-driven charge separation in modern photosystems. This provides a plausible evolutionary bridge between geochemical and biochemical oxygen production, supporting the central hypothesis of this paper: that photosynthetic oxygen evolution may have inherited functional elements from ancient mineral-based photochemistry (A). Gibbs standard free energy of H_2O and HCO_3^- as substrates of oxygen evolution, under thermodynamic equilibrium, respectively (B) (Dismukes et al. 2001)

3 Potential ancestor of Photosystem II

Photosynthetic O_2 evolution is catalyzed by the Mn_4CaO_5 cluster in PSII of cyanobacteria and photosynthetic eukaryotes, facilitated by a suite of enzymes and proteins (Cardona et al., 2019). The Mn_4CaO_5 cluster in PSII represents an extraordinarily efficient oxygen-evolving complex, which has been pivotal in elevating atmospheric oxygen concentrations by six orders of magnitude (Catling and Zahnle, 2020). This raises an intriguing question: How did the process of oxygen production evolve from inefficient geological mechanisms to the highly efficient photosynthetic oxygen evolution system? Focusing solely on the Mn_4CaO_5 oxygen-evolving

cluster in PSII and setting aside the evolution of other associated enzymes and proteins, we propose that the precursor to this cluster could be carbonic anhydrase.

Carbonic Anhydrases (EC 4.2.1.1) constitute a vast enzyme family with over 2,000 identified members in diverse organisms, including bacteria, archaea, fungi, plants, and animals (Badger and Price, 1994; Moroney et al., 2001; Wu & Rao, 2023). These enzymes within a diverse superfamily of metalloenzymes facilitate the reversible CO₂ hydration to bicarbonate. Without CA, this typically takes around a minute, but with CA, the reaction time is drastically reduced to 10⁻⁶ seconds (Prince and Woolley, 1973). CAs, versatile biocatalysts, are crucial in various chemical and biochemical processes. Notably, transition metal-incorporating CAs not only supply protons and electrons but also exhibit redox functionalities (Mesbahuddin et al., 2021). This is why they are deemed precursors to PSII's Mn₄CaO₅ oxygen-evolving complex.

Thylakoid CA (tCA) and PSII exhibit significant functional parallels across various dimensions (Wu, 2021). Specific anions and cations critical for photosynthetic processes, such as Cl⁻, Ca²⁺, and Mn²⁺, influence both tCA and PS II activities comparably (Lu and Stemler, 2007; Stemler, 1986; 1997). High-intensity light inhibits the activity of both tCA and PS II, causing photoinhibition due to electron transport disruption (Kyle et al., 1984; Stemler, 1986). Moreover, far-red light enhances the activity of both tCA and the Hill reaction (Govindjee et al. 1960; Stemler, 1997). Crucially, tCA's sensitivity to alterations in ambient redox potential mirrors PS II's behavior (Bearden and Malkin, 1973; Moubarak-Milad and Stemler, 1994). PSII not only displays traits of photosynthetic O₂ evolution but also exhibits CA activity (Dai et al., 2001; Ignatov et al., 2011; Khristin et al., 2004; Koroidov et al., 2014; Shitov et al., 2025; Stemler, 1986). PSII encompasses both extrinsic and intrinsic CAs, which are inseparable from it (Enami et al., 2008; Hillier et al., 2006; Ignatov et al., 2011; Lu and Stemler, 2002; Moskvina et al., 2004; Shitov et al., 2009; 2025; Villarejo et al., 2002). PS II's oxygen-evolving activity, linked to intrinsic CA, is clearly associated with the Mn cluster, while its CA activity is independent of the Mn cluster's presence (Shitov et al., 2009). Moreover, CA(Mn), where manganese replaces zinc at the catalytic site, has demonstrated the capacity to produce O₂ in the presence of H₂O₂ and HCO₃⁻ (Okrasa and Kazlauskas, 2006). Hence, it is reasonable to hypothesize that the integration of manganese into PSII's intrinsic carbonic anhydrase (CA) is pivotal for photosynthetic O₂ evolution, with the CA at the manganese-substituted active site potentially serving as the precursor to PSII's Mn₄CaO₅ O₂-evolving complex.

To date, nine genetically distinct CA families have been identified, each characterized by unique amino acid sequences. These families are classified as α -, β -, γ -, δ -, ϵ -, ζ -, η -, θ -, and ι -CAs. Despite functional similarities, they lack significant sequence identity and have evolved independently (Wu and Rao, 2023). The γ -CA, originating 3-4 Ga ago, epitomizes Earth's earliest CA form (Hewett-Emmett and Tashian, 1996; Tripp et al., 2004). The enzyme's active center metal ion is Fe(II), aligning its existence closely with the genesis of life itself (Knoll and Nowak, 2017). Non-biological oxygen production preceded the advent of primitive photosynthetic cyanobacteria by roughly 1 Ga, albeit in minuscule quantities (Des Marais, 2000; Fischer et al., 2016).

Approximately 3.8 Ga, oceans were largely anoxic, with Fe(II) levels 10,000-100,000 times higher than Mn(II) (Anbar, 2008). Despite Fe(II) and Mn(II)'s similar ionic radii, Mn rarely substitutes for Fe in γ -CA, leading to the scarcity of γ -CA[Mn] in the early Archean eon. This precluded the use of Mn-based redox reactions for phototrophy, allowing only photoferrotrophic organisms to emerge (Czaja et al., 2013). As γ -CA[Mn] levels progressively increased, oxygen-evolving photosynthetic efficiency gradually enhanced. However, the inefficient oxygen evolution by γ -CA[Mn] led to the evolution of solely phototrophic organisms during the mid-Archaean era (Tice and Lowe, 2004).

In the early Archean, seawater pH was between 6.5 and 7.0 (Halevy and Bachan, 2017). Without CA, CO₂ hydrolysis in seawater to bicarbonate is severely constrained. Analogous to the Mn₄CaO₅ cluster's photosynthetic O₂ evolution, a γ -CA with trace γ -CA[Mn] complex fulfills multiple key roles. Primarily, it functions as a CA, catalyzing CO₂ hydrolysis to produce substantial bicarbonate. Moreover, with ample bicarbonate, a minor Mn fraction in γ -CA[Mn] reacts to form Mn(II)-bicarbonate complexes (Baranov et al., 2000; 2004; Khorobrykh et al., 2008). This interaction reduces the system's redox potential from 1.19 V to 0.52-0.68 V, thereby initiating manganese oxidation over iron, as the redox potential for trivalent iron is 0.77 V (Lovyagina and Semin, 2022). Ultimately, within the Mn(III, IV)-bicarbonate complex, enzymatic release of bicarbonate ions leads to their subsequent oxidation, liberating O₂ and CO₂ (Stemler, 1986). Upon comparing the redox potentials, the thermodynamic favorability of bicarbonate decomposition versus Mn(II) oxidation to Mn(III,IV) is evident (Dasgupta et al., 2006; Kozlov et al., 2004; 2010; Yun et al., 1997). Notably, similar processes occur in PS II (Dai et al., 2001; Klimov et al., 1995; Shevela et al., 2008).

Rock weathering significantly contributes Mn²⁺ to Earth's aquatic systems; elevated Mn²⁺

levels are observed in both surface and deep waters of Archaean basins (Fischer et al., 2015). Mn(II) oxidation necessitates robust oxidants, e.g., O₂ or its derivatives, for redox cycling. This process occurs at a notably slow pace, even under oxygen-rich conditions, especially without biocatalysts (Morgan 2005). Mn-rich Fe formations were found in the Koegas Subgroup, Griqualand West structural sub-basin, Kaapvaal Craton, South Africa, dating back ~2.415 Ga (Johnson et al., 2013). A Mn-enriched thin horizon was also identified in the Turee Creek strata of Western Australia, dating to the same period (Williford et al., 2011). Elevated Mn levels, relative to other Archaean successions, were detected in early Witswatersrand and Mozaan Basin sediments, South Africa, dating to ~2.9 Ga (Planavsky et al., 2014; Smith and Beukes, 2023). Evidently, biocatalysts akin to γ -CA[Mn] likely facilitated the manganese oxidation cycle during the Archaean era. With γ -CA[Mn]'s enhanced bicarbonate decomposition capacity, increased manganese oxidation ensues, resulting in elevated manganese levels in sediments. This, in turn, may explain that the Griqualand West sub-basin's sediments (~2.415 Ga) exhibit higher manganese levels than those of the older Witswatersrand and Mozaan Basins (~2.9 Ga).

CA is crucial for calcium carbonate deposition (Kim et al., 2012; Rodriguez et al., 2019). Similarly, the γ -CA[Mn]-like enzyme, facilitating bicarbonate decomposition and oxygen release, also fosters carbonate precipitation. Organic carbon signatures in 3.8-Ga-old meta-carbonate rocks from West Greenland's Archaean Isua supracrustal belt have been identified (Schidlowski, 1988), along with clusters of organic microspheres in thin stromatolite layers from the 2.724-Ga-old Tumbiana Formation of Australia's Fortescue Group (Lepot et al., 2008). Considering the γ -CA[Mn]-like enzyme's capacity to break down bicarbonate and release O₂, it is reasonable to deduce that this organic carbon was not generated by cyanobacteria-like photosynthetic organisms. Instead, organic carbon in meta-carbonates is likely derived from geological processes, whereas that in stromatolites may have been produced by macromolecules akin to γ -CA[Mn]. Thus, despite the presence of organic carbon in 2.5 Ga-old stromatolite carbonates, no cyanobacteria-like microfossils have been identified within these structures (Fischer et al., 2016). Fig. 7 depicts the hypothesis that γ -CA[Mn] enzyme may serve as a precursor to primitive PSII, offering a logical rationale for these observations. Nonetheless, further chemical, geological, and biological evidence is required to validate this hypothesis conclusively.

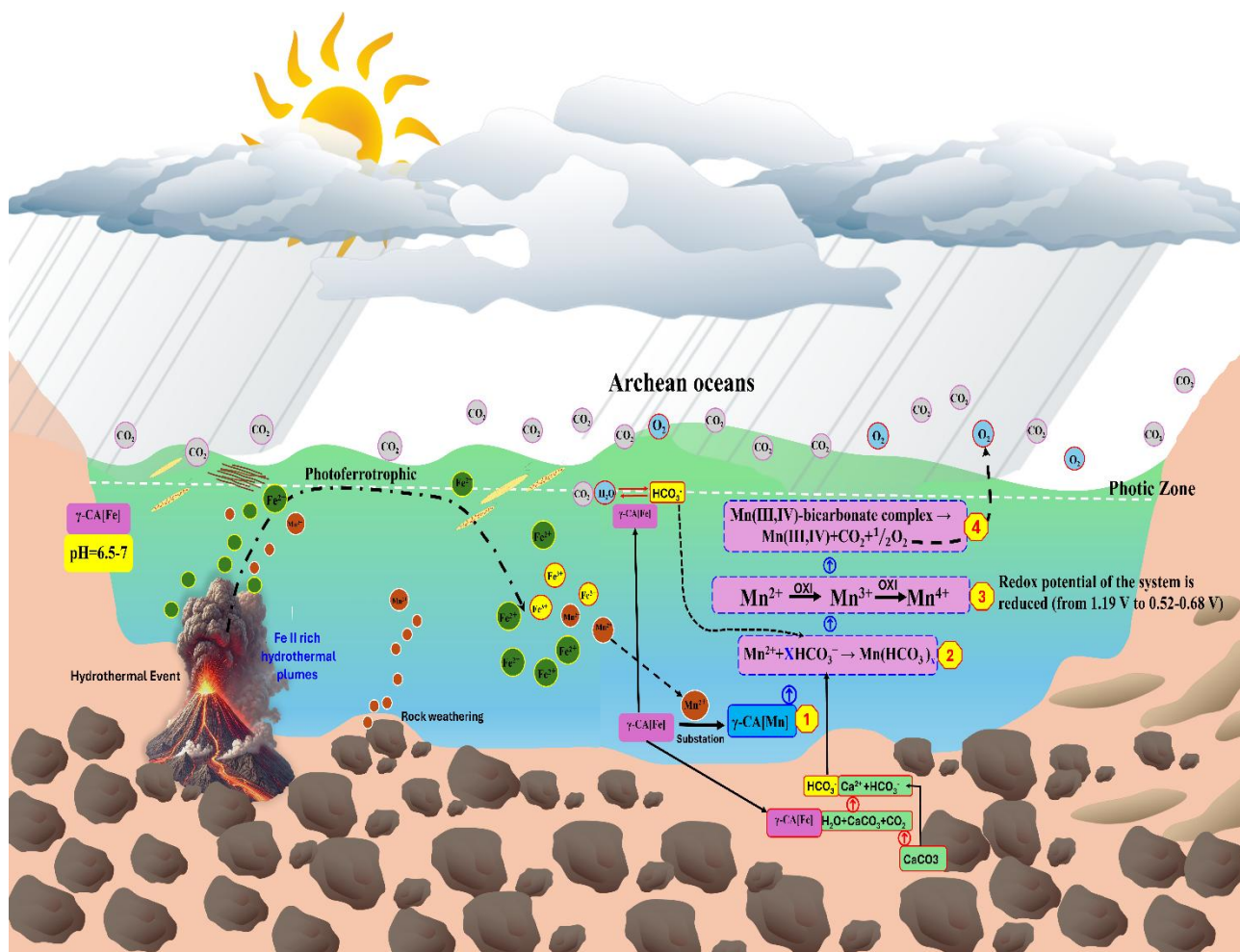


Figure 7. Illustration of an early Archean ocean ecosystem where hydrothermal vents release large amounts of Fe^{2+} (ferrous iron), which is oxidized to Fe^{3+} (ferric iron) through photoferrotrophy by early microorganisms using sunlight. This oxidation process, along with Mn^{2+} cycling, leads to the substitution of Fe by Mn in enzyme complexes like $\gamma\text{-CA}[\text{Mn}]$, potentially ancestral to Photosystem II. These processes contribute to carbonate rock dissolution, CO_2 cycling, and oxygen release, gradually reducing the system's redox potential. Overall, this ecosystem reflects the interplay between iron, manganese, and carbon cycles, laying the groundwork for oxygenic photosynthesis and early atmospheric oxygenation.

4 Two-substrate photosynthetic oxygen evolution

Both geological O_2 evolution and $\gamma\text{-CA}[\text{Mn}]$ -analogous O_2 production likely involve the thermodynamically favorable decomposition of bicarbonate to release O_2 . However, despite the

rapid isotopic exchange between bicarbonate and water during photosynthesis, our recent experiments using dual-element (C,O) bidirectional stable isotope labeling bicarbonate indicate that photosynthetic O₂ evolution is a dual-substrate process. Specifically, bicarbonate is involved in the S₄→S₀ transition of the Kok–Joliot cycle, while water participates in the S₂→S₃ transition shown in Fig.8 (Guo et al.,2024). Since the photolysis of bicarbonate requires only two-thirds of the free energy needed for water photolysis, it proceeds at a significantly faster rate (Dismukes et al., 2001). Consequently, the S₃→S₄→S₀ transition features a low energy barrier and an ultra-short-lived S₄ state, posing challenges for detection with current instruments (Guo et al.,2024; Wu and Guo, 2024).

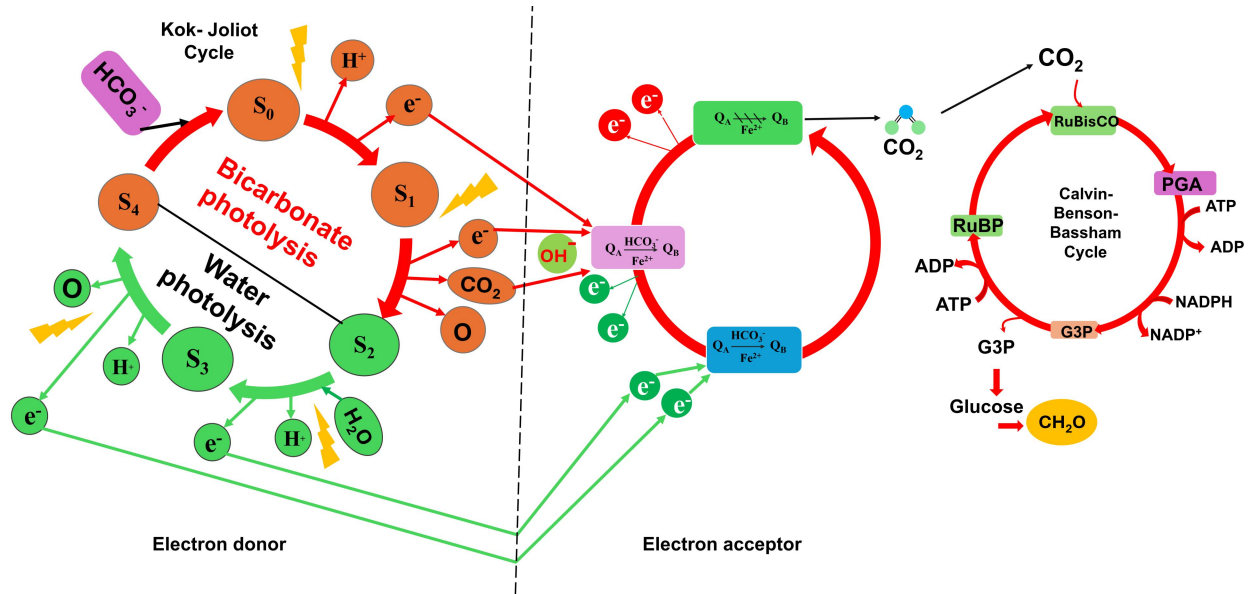


Figure 8. Schematic representation of bicarbonate and water photolysis as electron donors driving photosynthetic carbon fixation. Bicarbonate photolysis, which requires lower energy than water photolysis, facilitates the release of electrons and the production of CO₂, which becomes the exclusive carbon source for assimilation in the Calvin-Benson-Bassham cycle. CO₂ is incorporated via RuBisCO into the cycle, enabling the production of G3P and ultimately glucose, thereby linking light-driven electron flow with global biogeochemical and elemental cycling. This integrated mechanism underscores the critical role of bicarbonate in sustaining photosynthetic energy conversion and carbon assimilation on Earth (adapted from Guo et al.,2024).

Although photosynthetic O₂ evolution can be replicated *in vitro*, it markedly differs from that

in vivo. Photosynthetic O₂ evolution in chloroplast thylakoid membranes is regulated by physiological factors including pH and redox potential. Hydroxylamine disruption and PSII crystallography studies conducted *in vitro* necessitate analysis considering normal physiological parameter (Wu and Guo, 2024). At pH 6.0, hydroxylamine-induced disruption of PSII's oxygen-evolving center didn't result in CO₂ release (Shevela et al., 2008; Ulas et al., 2008), but this doesn't conclusively refute bicarbonate binding sites in PSII. This is because prior to hydroxylamine's interaction with the oxygen-evolving center, bicarbonate dissociation was already triggered by weak acid treatment. In fact, both tCA and PSII can actively regulate the pH and redox potential of their surrounding environment *in vivo* (Brinkert et al., 2016; Moubarak-Milad and Stemler, 1994). Under normal physiological conditions, bicarbonate binding to the oxygen-evolving complex of PSII is facilitated. This binding is influenced by both crystal formation conditions and the plant's physiological state. Bicarbonate binding to the oxygen-evolving complex is absent in PSII crystals grown at pH < 7 (Bhowmick et al. 2023; Lol et al., 2005; Umena et al., 2011). However, bicarbonate binding to the oxygen-evolving center was noted in PSII crystals crystallized *in vitro* at pH 7.5 (Ferreira et al., 2004). This phenomenon can be explained as follows: at pH < 7.0, the bicarbonate binding force to the oxygen-evolving complex of PSII is significantly reduced. Despite potential binding events, their detection is challenging due to the ultra-short lifespan of the S₄ transition state within the Kok-Joliot cycle. In contrast, at pH 7.5, the likelihood of bicarbonate binding to the oxygen-evolving complex increases substantially, making it more readily observable.

The long-standing belief that bicarbonate does not serve as a substrate for oxygen evolution in photosynthesis, backed by experiments with ¹⁸O-labeled bicarbonate and PSII crystallography, is increasingly contested. However, recent studies suggest bicarbonate is crucial for photosynthetic O₂ evolution. Besides the bicarbonate effect and the thermodynamic advantages of bicarbonate photolysis, photosynthetic oxygen evolution in chloroplasts appears to be dependent on CO₂ (Walker et al., 1971). Bicarbonate acts as a crucial ligand in forming the manganese cluster on PSII's electron donor side (Klimov et al., 1995), functioning as both an electron donor and proton acceptor within the photosynthetic oxygen evolution center (Allakhverdiev et al., 1997; Dai et al., 2001). Moreover, bicarbonate drives O₂ and CO₂ generation under illumination (Dai et al., 2001), with CO₂ formation from bicarbonate documented on both the electron donor and acceptor sides of PSII (Shevela et al., 2020). Significantly, bicarbonate binding sites have been identified both on

the electron acceptor side of PSII and the electron donor side at the core of oxygen evolution (Stemler and Castelfranco, 2023). Conclusively, the above evidence supports that PSII's electron donor side facilitates a photosynthetic oxygen evolution reaction, employing bicarbonate as the substrate: $\text{HCO}_3^- \rightarrow 1/2 \text{O}_2 + 2\text{e}^- + \text{H}^+ + \text{CO}_2$.

Water, another substrate in the photosynthetic O_2 evolution, likely evolved in plants due to reduced inorganic carbon (bicarbonate/ CO_2) availability. During the Archean eon (~2.5 Ga ago), atmospheric CO_2 levels ranged from 0.9 to 900 kPa, contrasting sharply with the period from 75 Ma ago to the pre-industrial Holocene, where CO_2 concentrations hovered around 0.03 kPa. Similarly, the bicarbonate levels in Archean seawater varied between 15 and 15,000 mM, whereas from 75 Ma ago to the Holocene, bicarbonate levels in seawater were reduced to just two mM (Dismukes et al., 2001).

The dissolution of silicate and carbonate rocks is Earth's primary geological process for CO_2 sequestration. Silicate rock dissolution occurs through the reaction: $[\text{CO}_2 + \text{Ca}(\text{Mg})\text{SiO}_3 \rightarrow \text{Ca}(\text{Mg})\text{CO}_3 + \text{SiO}_2]$. Carbonate rock dissolution, or karstification, follows the equation: $[\text{Ca}(\text{Mg})\text{CO}_3 + \text{H}_2\text{O} + \text{CO}_2 \rightleftharpoons \text{Ca}(\text{Mg})^{2+} + 2\text{HCO}_3^-]$. The interplay between karstification and photosynthesis is crucial for maintaining the equilibrium of inorganic carbon in the atmosphere and oceans (Wu and Rao, 2023). Throughout geological history, elevated atmospheric CO_2 levels have coincided with reduced photosynthetic activity. For example, early Paleozoic's high CO_2 was linked to terrestrial plants' absence, whereas Permian-Carboniferous's lower CO_2 levels corresponded with vascular plants' emergence, development, and proliferation (Bernier, 1990; Knoll et al., 2017; Moulton and Bernier, 1998). The rise of efficient eukaryotic photosynthetic organisms 75 Ma ago necessitated coping with scarce inorganic carbon (bicarbonate/ CO_2). Consequently, these organisms evolved the capability to leverage abundant water to evolve oxygen and enhance inorganic carbon assimilation. These photosynthetic organisms have undergone evolutionary milestones, encompassing the development of PS I and PS II, the evolution of the photosynthetic oxygen-evolving center and associated proteins, and the emergence of electron transport and photosynthetic phosphorylation mechanisms (Badger and Price, 1994; Fischer et al., 2016; Hohmann-Marriott and Blankenship, 2011; Xiong and Bauer, 2002). These evolutionary adaptations, which facilitate the release of oxygen from water, likely enhanced photosynthesis efficiency by significantly boosting oxygen production under conditions of insufficient inorganic carbon in the environment.

Optimal energy use and photosynthetic efficiency are achieved through equivalent photolysis of HCO_3^- and H_2O , exemplifying the coupling between karstification and photosynthesis shown in Fig.9. Since photolysis of bicarbonate requires less energy than water photolysis, it results in CO_2 being the sole carbon source for photosynthetic inorganic carbon assimilation. This CO_2 is then fully incorporated into the Calvin-Benson-Bassham cycle by RuBisCO, driving the biogeochemical cycle and maintaining elemental equilibrium on Earth shown in Fig.8 (Wu and Rao, 2023).

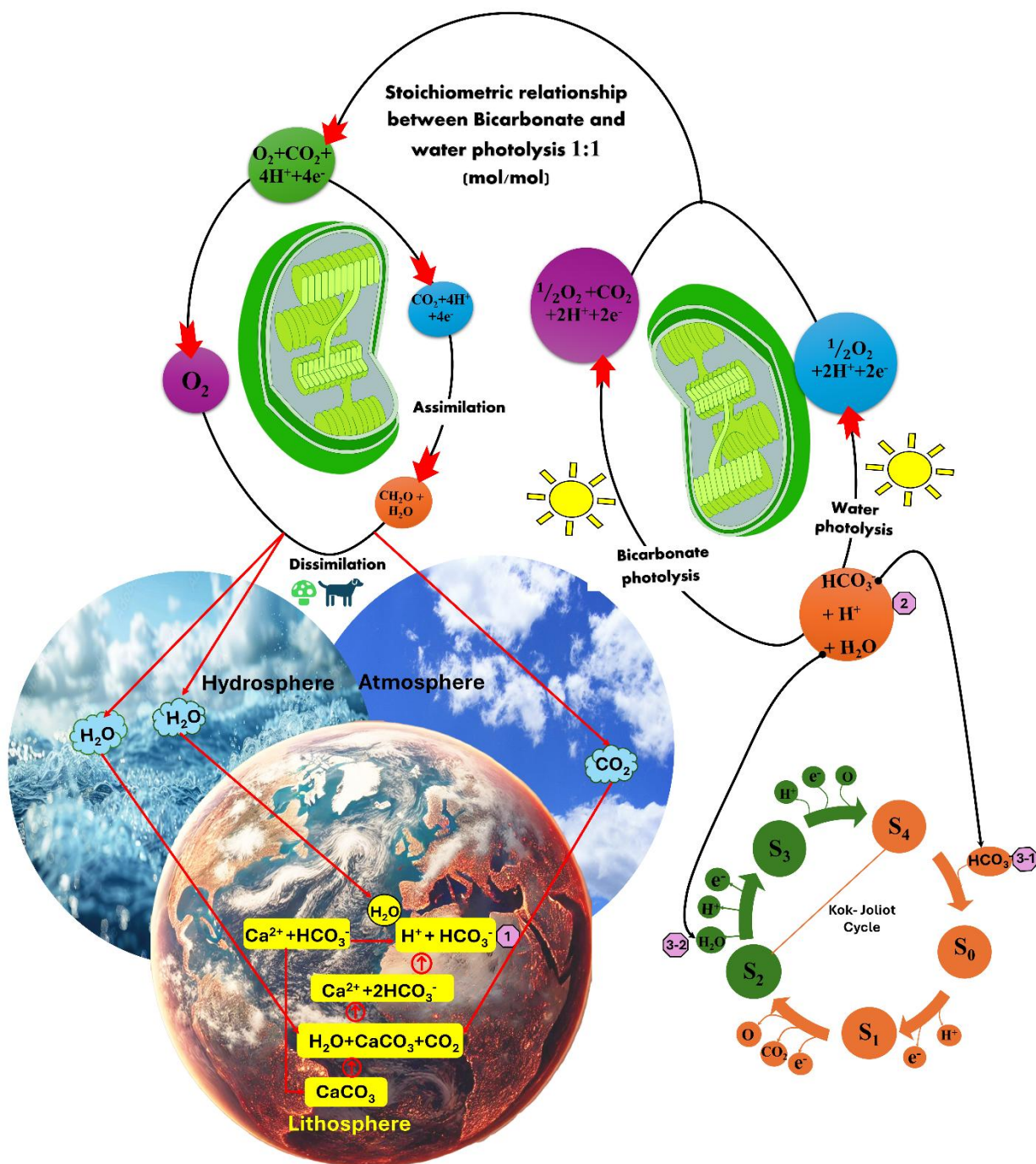


Figure 9. The dual-substrate nature of photosynthetic oxygen evolution, involving both HCO_3^- and H_2O , with bicarbonate playing a key role in the $\text{S}_4 \rightarrow \text{S}_0$ transition and water in the $\text{S}_2 \rightarrow \text{S}_3$ transition of the Kok-Joliot cycle. Bicarbonate photolysis is more energy-efficient than water, enabling faster oxygen release. The process operates in a 1:1 molar ratio between bicarbonate and water photolysis, driving oxygen and CO_2 production. The image also connects this mechanism to

Earth's geological carbon cycles, highlighting how the dissolution of carbonate and silicate rocks, coupled with photosynthesis, regulates atmospheric carbon levels. This model reflects the evolutionary adaptation of early photosynthetic organisms to utilize water and bicarbonate for oxygen generation, which plays a critical role in maintaining Earth's elemental balance.

Investigating PSII's dual-substrate nature is pivotal for advancing artificial photosynthetic reactors, which could bolster carbon sequestration and oxygen production to mitigate climate change. Insights from this research may also guide agricultural innovations, enhancing plant photosynthesis and resilience to high CO₂ levels, emulating ancient photosynthetic adaptations.

Conclusions

The complex biochemical intricacies of modern photosynthesis may trace back to Earth's primordial geological processes, providing a transformative perspective on the continuum between inorganic and organic evolution. Building upon this profound insight, we propose that the biochemical mechanism responsible for photosynthetic oxygen evolution in plants evolved gradually from simpler, abiotic geological oxygen production processes. Origins of bicarbonate photolysis in photosynthetic O₂ evolution may trace back to early abiotic O₂-generating systems. This hypothesis is a potentially groundbreaking perspective on the evolution of life, suggesting that key aspects of photosynthesis, once believed to be exclusive to biological systems, may have originated in pre-biological processes. This concept underscores the seamless transition from inorganic to organic processes in nature. Validating this hypothesis would profoundly impact our comprehension of life's origins and the evolution of intricate biochemical processes. It would also imply that the mechanisms underlying photosynthesis are deeply rooted in ancient abiotic processes. Further research is essential to substantiate this claim, but pursuing this line of inquiry could open new avenues for understanding the origins of photosynthesis and the intricate interplay between inorganic and organic chemistry in shaping Earth's biosphere.

Data availability: Data will be made available on request.

Authors' Contributions

Y.W. Conceptualization, writing raw manuscript, and validation, **M.A.** writing and review and

visualization, **C.L.** validation and revision. All authors have read and agreed to the published version of the manuscript.

Conflict of Interest: The authors declare no conflict of interest.

Acknowledgements

We extend our sincere gratitude to G. Govindjee and A. Stemler for their invaluable support, insightful comments, and assistance in revising this manuscript. Their contributions enhanced the quality of our work.

References

- Allakhverdiev, S. I., Yruela, I., Picorel, R.: Bicarbonate is an essential constituent of the water-oxidizing complex of photosystem II. *Proc. Natl Acad. Sci. USA*, 94(10), 5050-5054. <https://doi.org/10.1073/pnas.94.10.5050>, 1997.
- Anbar, A. D.: Elements and evolution. *Science*, 322(5907), 1481–1483. <https://doi.org/10.1126/science.1163100>, 2008.
- Anbar, A. D., Duan, Y., Lyons, T. W., Arnold, G. L., Kendall, B., Creaser, R. A., Kaufman, A. J., Gordon, G. W., Scott, C., and Garvin, J.: A whiff of oxygen before the great oxidation event? *Science*, 317, 1903–1906. <https://doi.org/10.1126/science.1140325>, 2007
- Badger, M. R., and Price, G. D. : The role of carbonic anhydrase in photosynthesis. *Annu. Rev. Plant Physiol.*, 45, 369–392. <https://doi.org/10.1146/annurev.pp.45.060194.002101>, 1994.
- Baranov, S. V, Ananyev, G. M., Klimov, V. V, & Dismukes, G. C.: Bicarbonate accelerates assembly of the inorganic core of the water - oxidizing complex in manganese - depleted photosystem II: A proposed biogeochemical role for atmospheric carbon dioxide in oxygenic photosynthesis. *Biochemistry*, 39(20), 6060–6065. <https://doi.org/10.1021/bi992682c>, 2000.
- Baranov, S. V, Tyryshkin, A. M., Katz, D., Dismukes, G. C., Ananyev, G. M., and Klimov, V. V.: Bicarbonate is a native cofactor for assembly of the manganese cluster of the photosynthetic water oxidizing complex. Kinetics of reconstitution of O₂ evolution by photoactivation. *Biochemistry*, 43(7), 2070–2079. <https://doi.org/10.1021/bi034858n>, 2004.

510 Bearden, A. J., and Malkin, R.: Oxidation-reduction potential dependence of low - temperature
 511 photoreactions of chloroplast photosystem II. *Biochim. Biophys. Acta - Bioenergetics*, 325(2),
 512 266–274. [https://doi.org/10.1016/0005-2728\(73\)90102-3](https://doi.org/10.1016/0005-2728(73)90102-3), 1973.

513 Berner, R. A.: Atmospheric carbon dioxide levels over Phanerozoic time. *Science*, 249(4975),
 514 1382–1386. <https://doi.org/10.1126/science.249.4975.1382>, 1990.

515 Berner, R. A.: Atmospheric oxygen over Phanerozoic time. *Proc. Natl Acad. Sci. USA*, 96(20),
 516 10955–10957. <https://doi.org/10.1073/pnas.96.20.10955>, 1999.

517 Bhowmick, A., Hussein, R., Bogacz, I., Simon, P. S., Ibrahim, M., Chatterjee, R., Doyle, M. D.,
 518 Cheah, M. H., Fransson, T., and Chernev, P. : Structural evidence for intermediates during O₂
 519 formation in photosystem II. *Nature*, 617, 629–636. <https://doi.org/10.1038/s41586-023-06038-z>,
 520 2023.

521 Brasier, M. D., Green, O. R., Jephcoat, A. P., Kleppe, A. K., Van Kranendonk, M. J., Lindsay, J. F.,
 522 Steele, A., and Grassineau, N. V.: Questioning the evidence for Earth’s oldest fossils. *Nature*, 416,
 523 76–81. <https://doi.org/10.1038/416076a>, 2002.

524 Brasier, M. D., Green, O. R., Lindsay, J. F., McLoughlin, N., Steele, A., and Stoakes, C. : Critical
 525 testing of Earth’s oldest putative fossil assemblage from the ~3.5 Ga Apex chert, Chinaman Creek,
 526 Western Australia. *Precambrian Res.*, 140(1-2), 55–102.
 527 <https://doi.org/10.1016/j.precamres.2005.06.008>, 2005.

528 Brinkert, K., De Causmaecker, S., Krieger-Liszkay, A., Fantuzzi, A., and Rutherford, A. W.:
 529 Bicarbonate - induced redox tuning in Photosystem II for regulation and protection. *Proc. Natl*
 530 *Acad. Sci. USA*, 113(43), 12144–12149. <https://doi.org/10.1073/pnas.1608862113>, 2016.

531 Cardona, T., Sánchez-Baracaldo, P., Rutherford, A. W., and Larkum, A. W.: Early Archean
 532 eonorigin of Photosystem II. *Geobiology*, 17(2), 127–150. <https://doi.org/10.1111/gbi.12323>, 2019.

533 Catling, D. C., and Zahnle, K. J.: The Archean eon atmosphere. *Sci. Adv.*, 6(9), eaax1420.
 534 <https://doi.org/10.1126/sciadv.aax1420>, 2020.

535 Crowe, S. A., Døssing, L. N., Beukes, N. J., Bau, M., Kruger, S. J., Frei, R., and Canfield, D. E.:
 536 Atmospheric oxygenation three billion years ago. *Nature*, 501(7468), 535–538,
 537 <https://doi.org/10.1038/nature12426>, 2013.

538 Czaja, A. D., Johnson, C. M., Beard, B. L., Roden, E. E., Li, W., and Moorbath, S.: Biological Fe
 539 oxidation controlled deposition of banded iron formation in the ca. 3770 Ma Isua Supracrustal

540 Belt (West Greenland). *Earth Planet Sci. Lett.*, 363, 192–203.
 541 <https://doi.org/10.1016/j.epsl.2012.12.025>, 2013.

542 Dai, X., Yu, Y., Zhang, R., Yu, X., He, P., and Xu, C.: Relationship among photosystem II carbonic
 543 anhydrase, extrinsic polypeptides and manganese cluster. *Chin. Sci. Bull.* 46, 406–408,
 544 <https://doi.org/10.1007/BF03183276>, 2001.

545 Dasgupta, J., Tyryshkin, A. M., Kozlov, Y. N., Klimov, V. V, and Dismukes, G. C.. Carbonate
 546 complexation of Mn^{2+} in the aqueous phase: redox behavior and ligand binding modes by
 547 electrochemistry and EPR spectroscopy. *J. Phys. Chem. B*, 110(10), 5099–5111.
 548 <https://doi.org/10.1021/jp055213v>, 2006

549 Des Marais, D. J.: When did photosynthesis emerge on Earth? *Science*, 289(5485), 1703–1705.
 550 <https://doi.org/10.1126/science.289.5485.1703>, 2000.

551 Dismukes, G. C., Klimov, V. V, Baranov, S. V, Kozlov, Y. N., DasGupta, J., and Tyryshkin, A.:
 552 The origin of atmospheric oxygen on Earth: the innovation of oxygenic photosynthesis. *Proc. Natl*
 553 *Acad. Sci. USA*, 98(5), 2170–2175. <https://doi.org/10.1073/pnas.061514798>, 2001.

554 Enami, I., Okumura, A., Nagao, R., Suzuki, T., Iwai, M., and Shen, J.-R.: Structures and functions
 555 of the extrinsic proteins of photosystem II from different species. *Photosynth. Res.*, 98(1-3), 349–
 556 363. <https://doi.org/10.1007/s11120-008-9343-9>, 2008.

557 Ferreira, K. N., Iverson, T. M., Maghlaoui, K., Barber, J., and Iwata, S.: Architecture of the
 558 photosynthetic oxygen-evolving center. *Science*, 303(5665), 1831–1838.
 559 <https://doi.org/10.1126/science.1093087>, 2004.

560 Fischer, W. W., Hemp, J., and Johnson, J.: Evolution of oxygenic photosynthesis. *Annu. Rev. Earth*
 561 *Planet Sci.*, 44, 647–683. <https://doi.org/10.1146/annurev-earth-060313-054810>, 2016.

562 Fischer, W. W., Hemp, J., and Johnson, J. E.: Manganese and the evolution of photosynthesis. *Orig.*
 563 *Life Evol. Biosph.*, 45(3), 351–357. <https://doi.org/10.1007/s11084-015-9442-5>, 2015.

564 Govindjee, R., Thomas, J. B. and Rabinowitch, E.: “Second Emerson Effect” in the Hill reaction
 565 of *Chlorella* cells with quinone as oxidant. *Science* 132(3424), 421.
 566 <https://doi.org/10.1126/science.132.3424.421>, 1960.

567 Guo, S., Wu, Y., and Aboueldahab, M. : Rapid oxygen isotopic exchange between bicarbonate and
 568 water during photosynthesis. *J. Photochem. Photobiol. B: Biol.*, 255, 112924.
 569 <https://doi.org/10.1016/j.jphotobiol.2024.112924>, 2024.

570 Halevy, I., and Bachan, A.:The geologic history of seawater pH. *Science*, 355(6329), 1069–1071.
571 <https://doi.org/10.1126/science.aal4151>, 2017.

572 Hewett-Emmett, D., and Tashian, R. E.: Functional diversity, conservation, and convergence in
573 the evolution of the α -, β -, and γ -carbonic anhydrase gene families. *Mol. Phylogenet. Evol.*, 5(1),
574 50–77. <https://doi.org/10.1006/mpev.1996.0006>, 1996.

575 Hillier, W., McConnell, I., Badger, M. R., Boussac, A., Klimov, V. V, Dismukes, G. C., &
576 Wydrzynski, T.: Quantitative assessment of intrinsic carbonic anhydrase activity and the capacity
577 for bicarbonate oxidation in photosystem II. *Biochemistry*, 45(7), 2094–2102.
578 <https://doi.org/10.1021/bi051892o>, 2006.

579 Hohmann-Marriott, M. F., and Blankenship, R. E.: Evolution of photosynthesis. *Annu. Rev. Plant*
580 *Biol.*, 62, 515–548. <https://doi.org/10.1146/annurev-arplant-042110-103811>, 2011.

581 Holland, H. D.:The oxygenation of the atmosphere and oceans. *Philos. Trans. R. Soc. B Biol. Sci.*,
582 361(1470), 903–915. <https://doi.org/10.2337/diacare.26.3.905>, 2006.

583 Ignatova, L. K., Rudenko, N. N., Mudrik, V. A., Fedorchuk, T. P., and Ivanov, B. N.: Carbonic
584 anhydrase activity in *Arabidopsis thaliana* thylakoid membrane and fragments enriched with PSI
585 or PSII. *Photosynth. Res.*, 110(2), 89–98. <https://doi.org/10.1007/s11120-011-9699-0>, 2011.

586 Johnson, J. E., Webb, S. M., Thomas, K., Ono, S., Kirschvink, J. L., and Fischer, W.
587 W.:Manganese-oxidizing photosynthesis before the rise of cyanobacteria. *Proc. Natl Acad. Sci.*
588 *USA*, 110(28), 11238–11243. <https://doi.org/10.1073/PNAS.1305530110>, 2013.

589 Khorobrykh, A. A., Terentyev, V.V, Zharmukhamedov, S. K., and Klimov, V. V.:Redox interaction
590 of Mn–bicarbonate complexes with reaction centres of purple bacteria. *Philos. Trans. R. Soc. B*
591 *Biol. Sci.*, 363(1494), 1245–1251. <https://doi.org/10.1098/rstb.2007.2221>, 2008.

592 Khristin, M. S., Ignatova, L. K., Rudenko, N. N., Ivanov, B. N., and Klimov, V. V.:Photosystem II
593 associated carbonic anhydrase activity in higher plants is situated in core complex. *FEBS Lett.*,
594 577(1–2), 305–308. <https://doi.org/10.1016/j.febslet.2004.10.001>, 2004.

595 Kim, I. G., Jo, B. H., Dong, G. K., Chang, S. K., Choi, Y. S., Cha, H. J.: Biomineralization - based
596 conversion of carbon dioxide to calcium carbonate using recombinant carbonic
597 anhydrase. *Chemosphere*, 87(10), 1091-1096. <https://doi.org/10.1016/j.chemosphere.2012.02.003>.
598 2012.

599 Klimov, V.V, Allakhverdiev, S. I., Baranov, S.V, and Feyziev, Y. M.: Effects of bicarbonate and
 600 formate on the donor side of photosystem II. *Photosynth. Res.*, 46(1 - 3), 219–225.
 601 <https://doi.org/10.1007/BF00020434>, 1995.

602 Knoll, A. H., and Nowak, M. A.: The timetable of evolution. *Sci. Adv.*, 3(5), e1603076.
 603 <https://doi.org/10.1126/sciadv.1603076>, 2017.

604 Koroidov, S., Shevela, D., Shutova, T., Samuelsson, G., and Messinger, J.: Mobile hydrogen
 605 carbonate acts as proton acceptor in photosynthetic water oxidation. *Proc. Natl Acad. Sci. USA*
 606 111(17), 6299–6304. <https://doi.org/10.1073/pnas.1323277111>, 2014.

607 Kozlov, Y. N., Tikhonov, K. G., Zastrizhnaya, O. M., and Klimov, V. V.: pH dependence of the
 608 composition and stability of Mn (III)–bicarbonate complexes and its implication for redox
 609 interaction of Mn(II) with photosystem II. *J. Photochem. Photobiol. B: Biol.*, 101(3), 362–366.
 610 <https://doi.org/10.1016/j.jphotobiol.2010.08.009>, 2010.

611 Kozlov, Y. N., Zharmukhamedov, S. K., Tikhonov, K. G., Dasgupta, J., Kazakova, A. A.,
 612 Dismukes, G. C., and Klimov, V. V.: Oxidation potentials and electron donation to photosystem II
 613 of manganese complexes containing bicarbonate and carboxylate ligands. *Phys. Chem. Chem.*
 614 *Phys.*, 6, 4905–4911. <https://doi.org/10.1039/b406569g>, 2004.

615 Kyle, D. J., Ohad, I., and Arntzen, C. J. : Membrane protein damage and repair: selective loss of a
 616 quinone-protein function in chloroplast membranes. *Proc. Natl Acad. Sci. USA*, 81(13), 4070–
 617 4074. <https://doi.org/10.1073/pnas.81.13.4070>, 1984.

618 Lepot, K., Benzerara, K., Brown, G. E., and Philippot, P.: Microbially influenced formation of
 619 2,724-million-year-old stromatolites. *Nat. Geosci.* 1(2), 118–121. <https://doi.org/10.1038/ngeo107>,
 620 2008.

621 Lindell, D., Jaffe, J. D., Johnson, Z. I., Church, G. M., and Chisholm, S. W. Photosynthesis genes
 622 in marine viruses yield proteins during host infection. *Nature*, 438(7064), 86–89.
 623 <https://doi.org/10.1038/nature04111>, 2005.

624 Loll, B., Kern, J., Saenger, W., Zouni, A., and Biesiadka, J.: Towards complete cofactor
 625 arrangement in the 3.0 Å resolution structure of photosystem II. *Nature*, 438(7070), 1040–1044.
 626 <https://doi.org/10.1038/nature04224>, 2005.

627 Lovyagina, E. R., and Semin, B. K.: Competitive interaction of Mn (II) and Fe (II) cations with the
 628 high-affinity Mn-binding site of the photosystem II: evolutionary aspect. *Orig. Life Evol. Biosph.*,
 629 52(1 - 3), 113–128. <https://doi.org/10.1007/s11084-022-09625-8>, 2022.

630 Lu, A., Li, Y., Ding, H., Xu, X., Li, Y., Ren, G., Liang, J., Liu, Y., Hong, H., and Chen, N.:
 631 Photoelectric conversion on Earth's surface via widespread Fe-and Mn-mineral coatings. *Proc.*
 632 *Natl Acad. Sci. USA*, 116(20), 9741–9746. <https://doi.org/10.1073/pnas.1902473116>, 2019.
 633 Lu, Y. K., and Stemler, A. J.: Extrinsic photosystem II carbonic anhydrase in maize mesophyll
 634 chloroplasts. *Plant Physiol.*, 128(2), 643–649. [https://doi.org/10.1016/S0020-1383\(98\)00114-4](https://doi.org/10.1016/S0020-1383(98)00114-4),
 635 2002.
 636 Lu, Y. K., and Stemler, A. J.: Differing responses of the two forms of photosystem II carbonic
 637 anhydrase to chloride, cations, and pH. *Biochim. Biophys. Acta-Bioenergetics*, 1767(6), 633–638.
 638 <https://doi.org/10.1016/j.bbabi.2006.12.011>, 2007.
 639 Marshall, C. P., Emry, J. R., and Olcott Marshall, A.: Haematite pseudomicrofossils present in the
 640 3.5-billion-year-old Apex Chert. *Nat. Geosci.*, 4, 240–243. <https://doi.org/10.1038/ngeo1084>,
 641 2011.
 642 McCollom, T. M., and Seewald, J. S.: Carbon isotope composition of organic compounds
 643 produced by abiotic synthesis under hydrothermal conditions. *Earth Planet Sci. Lett.*, 243(1-2),
 644 74–84. <https://doi.org/10.1016/j.epsl.2006.01.027>, 2006.
 645 Mesbahuddin, M. S., Ganesan, A., and Kalyaanamoorthy, S.: Engineering stable carbonic
 646 anhydrases for CO₂ capture: A critical review. *Protein Eng. Des. Sel.*, 34, 1–12.
 647 <https://doi.org/10.1093/protein/gzab021>, 2021.
 648 Morgan, J. J.: Kinetics of reaction between O₂ and Mn (II) species in aqueous solutions. *Geochim.*
 649 *Cosmochim. Acta*, 69(1), 35–48. <https://doi.org/10.1016/j.gca.2004.06.013>, 2005.
 650 Moroney, J. V., Bartlett, S. G., Samuelsson, G.: Carbonic anhydrases in plants and algae: Invited
 651 review. *Plant Cell Environ.*, 24, 141–153. <https://doi.org/10.1111/j.1365-3040.2001.00669.x>, 2001.
 652 Moskvina, O. V., Shutova, T. V., Khristin, M. S., Ignatova, L. K., Villarejo, A., Samuelsson, G.,
 653 Klimov, V. V., & Ivanov, B. N. (2004). Carbonic anhydrase activities in pea
 654 thylakoids. *Photosynth. Res.*, 79, 93–100. <https://doi.org/10.1023/B:PRES.0000011925.93313.db>,
 655 2004
 656 Moubarak-Milad, M., and Stemler, A. J.: Oxidation-reduction potential dependence of
 657 photosystem II carbonic anhydrase in maize thylakoids. *Biochemistry*, 33(14), 4432–4438.
 658 <https://doi.org/10.1021/bi00180a042>, 1994.
 659 Moulton, K. L., and Berner, R. A.: Quantification of the effect of plants on weathering: studies in
 660 Iceland. *Geology*, 26(10), 895–898. [https://doi.org/10.1130/0091-7613\(1998\)0262.3.CO;2](https://doi.org/10.1130/0091-7613(1998)0262.3.CO;2), 1998.

661 Okrasa, K., and Kazlauskas, R. J.: Manganese-substituted carbonic anhydrase as a new
 662 peroxidase. *Chem. Eur. J.*, 12(6), 1587–1596. <https://doi.org/10.1002/chem.200501413>, 2006.

663 Pinti, D. L., Mineau, R., and Clement, V.: Hydrothermal alteration and microfossil artefacts of
 664 the 3,465-million-year-old Apex chert. *Nat. Geosci.*, 2(9), 640–643.
 665 <https://doi.org/10.1038/ngeo601>, 2009.

666 Planavsky, N. J., Asael, D., Hofmann, A., Reinhard, C. T., Lalonde, S. V, Knudsen, A., Wang, X.,
 667 Ossa Ossa, F., Pecoits, E., and Smith, A. J. B.: Evidence for oxygenic photosynthesis half a billion
 668 years before the Great Oxidation Event. *Nature Geoscience*, 7(4), 283–
 669 286. <https://doi.org/10.1038/ngeo2122>, 2014.

670 Prince, R. H., and Woolley, P. R.: On the mechanism of action of carbonic anhydrase. *Bioorg.*
 671 *Chem.*, 2(4), 337–344. [https://doi.org/10.1016/0045-2068\(73\)90034-5](https://doi.org/10.1016/0045-2068(73)90034-5), 1973.

672 Riding, R., Liang, L., and Fralick, P.: Oxygen-induced chemocline precipitation between Archean
 673 Fe-rich and Fe-poor carbonate seas. *Precambrian Res.*, 383, 106902.
 674 <https://doi.org/10.1016/j.precamres.2022.106902>, 2022.

675 Rodriguez, N., Navarro, C., Cizer, Ö., Kudłacz, K., Ibañez-Velasco, A., Ruiz-Agudo, C., Elert, K.,
 676 Burgos-Cara, A., and Ruiz-Agudo, E.: The multiple roles of carbonic anhydrase in calcium
 677 carbonate mineralization. *Cryst. Eng. Comm.*, 21, 7407–7423.
 678 <https://doi.org/10.1039/C9CE01544B>, 2019.

679 Rosing, M. T., and Frei, R.: U-rich Archean sea-floor sediments from Greenland – indications
 680 of >3700 Ma oxygenic photosynthesis. *Earth Planet Sci. Lett.*, 217(3 - 4), 237–244.
 681 [https://doi.org/10.1016/S0012-821X\(03\)00609-5](https://doi.org/10.1016/S0012-821X(03)00609-5), 2004.

682 Satkoski, A. M., Beukes, N. J., Li, W., Beard, B. L., Johnson, C. M.: A redox-stratified ocean 3.2
 683 billion years ago. *Earth Planet Sci. Lett.*, 430, 43–53.
 684 <https://doi.org/10.1016/j.epsl.2015.08.007>, 2015.

685 Schidlowski, M. A.: 3,800-million-year isotopic record of life from carbon in sedimentary
 686 rocks. *Nature*, 333, 313–318. <https://doi.org/10.1038/333313a0>, 1988.

687 Schirrmeister, B. E., de Vos, J. M., Antonelli, A., and Bagheri, H. C.: Evolution of multicellularity
 688 coincided with increased diversification of cyanobacteria and the Great Oxidation Event. *Proc.*
 689 *Natl Acad. Sci. USA*, 110(5), 1791–1796. <https://doi.org/10.1073/pnas.1209927110>. 2013.

690 Schopf, J. W.: Microfossils of the Early Archean Apex chert: new evidence of the antiquity of life.
 691 *Science*, 260(5108), 640–646. <https://doi.org/10.1126/science.260.5108.640>, 1993.

692 Schopf, J. W., and Packer, B. M.: Early Archean (3.3-billion to 3.5-billion-year-old) microfossils
 693 from Warrawoona Group, Australia. *Science*, 237(4810), 70–73.
 694 <https://doi.org/10.1126/science.11539686>, 1987.

695 Shevela, D., Do, H., Fantuzzi, A., Rutherford, A. W., and Messinger, J.: Bicarbonate-mediated
 696 CO₂ formation on both sides of photosystem II. *Biochemistry*, 59(26), 2442 - 2449.
 697 <https://doi.org/10.1021/acs.biochem.0c00208>, 2020.

698 Shevela, D., Su, J.-H., Klimov, V., and Messinger, J.: Hydrogencarbonate is not a tightly bound
 699 constituent of the water-oxidizing complex in photosystem II. *Biochim. Biophys. Acta (BBA)-*
 700 *Bioenergetics*, 1777(6), 532–539. <https://doi.org/10.1016/j.bbabi.2008.03.006>, 2008.

701 Shitov, A.V., Pobeguts, O. V, Smolova, T. N., Allakhverdiev, S. I., and Klimov, V. V.: Manganese-
 702 dependent carboanhydrase activity of photosystem II proteins. *Biochemistry (Moscow)*, 74, 509–
 703 517. <https://doi.org/10.1134/S0006297909050058>, 2009.

704 Shitov, A.V., Terentyev, V.V., and Govindjee G.: High and unique carbonic anhydrase activity of
 705 Photosystem II from *Pisum sativum*: Measurements by a new and very sensitive fluorescence
 706 method, *Plant Physiol. Biochem.*, 221, 109516, <https://doi.org/10.1016/j.plaphy.2025.109516>,
 707 2025.

708 Smith, A. J. B., and Beukes, N. J.: The paleoenvironmental implications of pre-Great Oxidation
 709 Event manganese deposition in the MesoArchean eonIjzermijn Iron Formation Bed, Mozaan
 710 Group, Pongola Supergroup, South Africa. *Precambrian Res.*, 384, 106922.
 711 <https://doi.org/10.1016/j.precamres.2022.106922>, 2023.

712 Stemler, A. J.:Carbonic anhydrase associated with thylakoids and photosystem II particles from
 713 maize. *Biochim. Biophys. Acta - Bioenergetics*, 850(1), 97–107. [https://doi.org/10.1016/0005-](https://doi.org/10.1016/0005-2728(86)90013-7)
 714 [2728\(86\)90013-7](https://doi.org/10.1016/0005-2728(86)90013-7), 1986.

715 Stemler, A. J.:The case for chloroplast thylakoid carbonic anhydrase. *Physiol. Plant*, 99(2), 348–
 716 353. <https://doi.org/10.1111/j.1399-3054.1997.tb05423.x>,1997.

717 Stemler, A. J., and Castelfranco, P. A.: The bicarbonate ion remains a critical factor in
 718 photosynthetic oxygen evolution. *Int. J. Life Sci.*, 12(2), 77–92. [https://doi.org/10.5958/2319-](https://doi.org/10.5958/2319-1198.2023.00009.X)
 719 [1198.2023.00009.X](https://doi.org/10.5958/2319-1198.2023.00009.X), 2023.

720 Sweetman, A. K., Smith, A. J., Jonge, D. S. W. D., Hahn, T., Schroedl, P., Silverstein, M.,
 721 Andrade, C., Edwards, R. L., Lough, A., J. M., Woulds, C.: Evidence of dark oxygen production

at the abyssal seafloor. *Nat. Geosci.*, 17, 737–739. <https://doi.org/10.1038/s41561-024-01480-8>, 2024.

Tice, M. M., and Lowe, D. R.: Photosynthetic microbial mats in the 3,416-Myr-old ocean. *Nature*, 431(7008), 549–552. <https://doi.org/10.1038/nature02888>, 2004.

Tripp, B. C., Bell, C. B., Cruz, F., Krebs, C., and Ferry, J. G.: A role for iron in an ancient carbonic anhydrase. *J. Biol. Chem.*, 279(8), 6683–6687. <https://doi.org/10.1074/jbc.M311648200>, 2004.

Ulas, G., Olack, G., and Brudvig, G. W.: Evidence against bicarbonate bound in the O₂-evolving complex of photosystem II. *Biochemistry*, 47(10), 3073–3075. <https://doi.org/10.1021/bi8000424>, 2008.

Umena, Y., Kawakami, K., and Shen, J. R.: Crystal structure of oxygen-evolving photosystem II at a resolution of 1.9 Å. *Nature*, 473, 55–60. <https://doi.org/10.1038/nature09913>, 2011.

Villarejo, A., Shutova, T., Moskvina, O., Forssén, M., Klimov, V. V., and Samuelsson, G.: A photosystem II-associated carbonic anhydrase regulates the efficiency of photosynthetic oxygen evolution. *EMBO J.* 21(8), 1930–1938. <https://doi.org/10.1093/emboj/21.8.1930>, 2002.

Walker, D. A., McCormick, A. V., and Stokes, D. M.: CO₂-dependent oxygen evolution by envelope - free chloroplasts. *Nature*, 233, 346–347. <https://doi.org/10.1038/233346a0>, 1971.

Walsh, M. M., and Lowe, D. R.: Filamentous microfossils from the 3,500-Myr-old Onverwacht Group, Barberton Mountain Land, South Africa. *Nature*, 314, 530–532. <https://doi.org/10.1038/314530a0>, 1985.

Wang, Y., Liu, X., Chen, T., Wang, H., Zhu, C., Yu, H., Song, L., Pan, X., Mi, J., and Lee, C.: An underwater flag-like triboelectric nanogenerator for harvesting ocean current energy under extremely low velocity condition. *Nano Energy*, 90, 106503. <https://doi.org/10.1016/j.nanoen.2021.106503>, 2021.

Wilde, S. A., Valley, J. W., Peck, W. H., and Graham, C. M.: Evidence from detrital zircons for the existence of continental crust and oceans on the Earth 4.4 Gyr ago. *Nature*, 409, 175–178. <https://doi.org/10.1038/35051550>, 2001.

Williford, K. H., Van Kranendonk, M. J., Ushikubo, T., Kozdon, R., and Valley, J. W.: Constraining atmospheric oxygen and seawater sulfate concentrations during Paleoproterozoic glaciation: In situ sulfur three-isotope microanalysis of pyrite from the Turee Creek Group, Western Australia. *Geochimica et Cosmochimica Acta*, 75(19), 5686–5705. <https://doi.org/10.1016/j.gca.2011.07.010>, 2011.

Wu, Y.:Is bicarbonate directly used as substrate to participate in photosynthetic oxygen evolution? *Acta Geochim.*, 40, 650–658. <https://doi.org/10.1007/s11631-021-00484-0>, 2021.

Wu, Y.:Combined effect of bicarbonate and water in photosynthetic oxygen evolution and carbon neutrality. *Acta Geochim.*, 42(1), 77–88. <https://doi.org/10.1007/s11631-022-00580-9>, 2023.

Wu, Y., and Guo, S.:The photosynthetic oxygen evolution does not exclude the important role and contribution of bicarbonate photolysis. *Acta Geochim.*, 43, 174–179. <https://doi.org/10.1007/10.1007/s11631-023-00649-z>, 2024.

Wu, Y., and Rao, S.:Root-derived bicarbonate assimilation in plants. Springer Nature Singapore. <https://doi.org/10.1007/978-981-99-4125-4>, 2023.

Xiong, J., and Bauer, C. E.: Complex evolution of photosynthesis. *Annu. Rev. Plant Biol.*, 53, 503–521. <https://doi.org/10.1146/annurev.arplant.53.100301.135212>, 2002.

Yun, K., Kazakova, A. A., and Klimov, V. V.:Changes in the redox potential and catalase activity of Mn²⁺ ions during formation of Mn-bicarbonate complexes. *Membr. Cell Biol.*, 11(1), 115–120. 1997.